Bioorganic & Medicinal Chemistry Letters xxx (2016) xxx–xxx

Contents lists available at ScienceDirect

Bioorganic & Medicinal Chemistry Letters

journal homepage: www.elsevier.com/locate/bmcl

# Synthesis and antibacterial evaluation of hamacanthin B analogues

Ahhyun Kim [a,†], Min Jeong Kim [a,†], Tae Hwan Noh [a], Jongki Hong [b], Yonghong Liu [c], Xiaoyi Wei [d], Jee H. Jung [a,*]

[a] College of Pharmacy, Pusan National University, Busan 609-735, Republic of Korea
[b] College of Pharmacy, Kyung Hee University, Seoul 130-701, Republic of Korea
[c] South China Sea Institute of Oceanology, Chinese Academy of Sciences, Guangzhou 510-650, PR China
[d] South China Botanical Garden, Chinese Academy of Sciences, Guangzhou 510-650, PR China

ARTICLE INFO

*Article history:*
Received 11 August 2016
Revised 25 August 2016
Accepted 30 August 2016
Available online xxxx

*Keywords:*
Hamacanthin B
Bisindole alkaloids
MRSA pyruvate kinase
Chiral separation

ABSTRACT

Hamacanthins are a class of antibacterial bisindole alkaloids isolated from marine sponges. Based on structure–activity relationships and in silico MRSA PK binding analysis of these bisindole alkaloids, the authors designed new hamacanthin B derivatives and evaluated their antibacterial activities against drug-resistant pathogens. Racemates of the synthetic products were resolved into their enantiomers by chiral separation using a cellulose column, and antibacterial activities were compared. Unsaturation of the central heterocyclic ring structure and bromine substitution at the indole moiety were found to enhance the antibacterial activities of hamacanthin B analogues.



Serious infections caused by pathogens that resist commonly used antibiotics have become a major global healthcare concern. Antibiotic resistance has now extended into the community, and causes severe infections that are difficult to diagnose and treat.[1,2] Furthermore, the problem posed by the explosive growth in the development of antimicrobial resistance has been made worse by a steady decrease in the numbers of new antibiotics approved over the last three decades. In fact, the annual mortality attributed to methicillin-resistant *Staphylococcus aureus* (MRSA) infection now exceeds that of AIDS in the USA and accounts for 18,000 deaths per annum,[3] and thus, there is an urgent need for efficient antibacterial agents against drug-resistant pathogens.

During our search for bioactive metabolites from marine sponges, we isolated hamacanthins and hamacanthin derivatives (Fig. 1) from the sponge *Spongosorites* sp.[4,5] Hamacanthins A (**2a**) and B (**4a**) and their analogues (**1a**, **2b**, **3a**, and **4c**) exhibited significant antibacterial activity against several human pathogens and MRSA strains,[4–7] and bromine substitution on the indole rings and 3,4-unsaturation of the piperazinone ring were found to improve antibacterial activity. Therefore, we synthesized further unsaturated ($\Delta^{3,5}$) analogues (**11a** and **11b**, Scheme 1), and compared their activities against those of saturated analogues (**12**–**13**). In addition, we explored relationships between molecular configurations and the antibacterial activities of these saturated analogues.

In a recent Letter,[7] the mechanism underlying the antibacterial effect of *cis*-3,4-dihydrohamacanthin B (**3a** = **13b**) was ascribed to the inhibition of methicillin-resistant *Staphylococcus aureus* pyruvate kinase (MRSA PK), which was also suggested to be a potential antimicrobial drug target. Pyruvate kinase (PK) is critical for bacterial survival, and it plays a major role in the regulation of carbohydrate metabolism by converting phosphoenolpyruvate to pyruvate and concurrently phosphorylating ADP to ATP.[8] The substrates and products of PK participate in a number of biosynthetic pathways, which places PK at a pivotal metabolic intersection. Accordingly, PK should be highly sensitive to mutation. Sequence alignments of MRSA and human PKs displayed notable divergence in domain C, which is involved in formation of small interfaces for ligand binding.[9] Furthermore, this divergence might endow different ligand selectivities to MRSA and mammalian PKs. In a co-crystal structure of **3a** and MRSA PK, **3a** bound to this small interface of MRSA PK tetramer.[7] H-bonds between the indole NH of **3a** and $Ser^{362}$ of chains A and B of MRSA PK are indicated in Figure 2A. Hydrophobic interactions between the indole moieties of **3a** and $Ile^{361}$ and $His^{365}$ of MRSA PK were prominent. Two bromine atoms of **3a** occupied a hydrophobic pocket formed by $Thr^{353}$, $Ser^{354}$, $Ala^{358}$, and $Leu^{370}$ of MRSA PK, and interestingly, the symmetric nature of this binding pocket was mirrored by the pseudo-symmetric properties of **3a** (Fig. 2A). A series of halogenated bisindoles modeled on the scaffold of **3a** were synthesized

* Corresponding author. Tel.: +82 51 510 2803; fax: +82 51 513 6754.
*E-mail address:* jhjung@pusan.ac.kr (J.H. Jung).
† These authors equally contributed to this work.

http://dx.doi.org/10.1016/j.bmcl.2016.08.095
0960-894X/

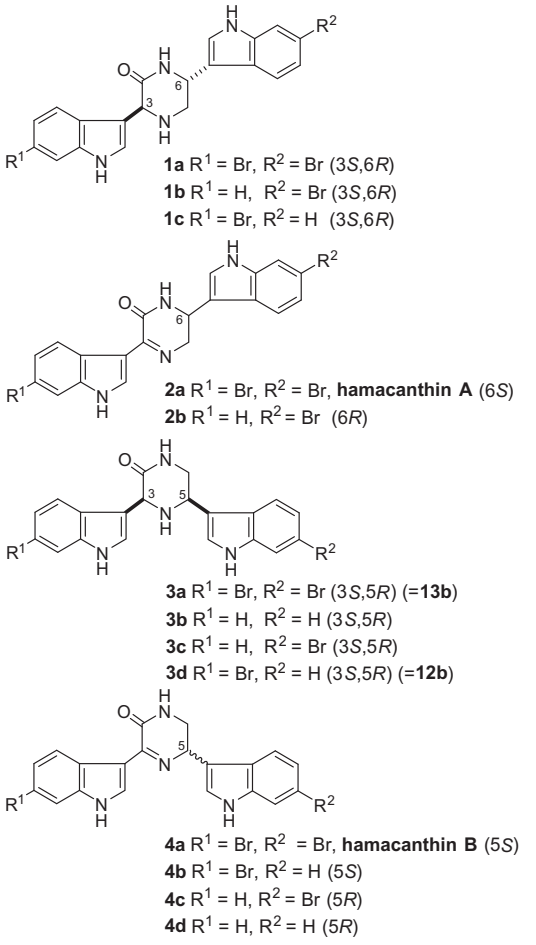


**Figure 1.** Hamacanthins A and B and their congeners isolated from the marine sponge *Spongosorites* sp.

and were found to inhibit MRSA PK, indicating that indole ring halogenation is essential for antibacterial activity.[10] The bisindole alkaloid deoxytopsentin, which has an imidazole central ring instead of the piperazinone ring of **3a**, was also subjected to SAR study due to its similar computed binding mode.[11]

In our preliminary in silico analysis, further unsaturated analogues (pyrazinones **11a** and **11b**) were found to bind to the same interface of MRSA PK tetramer in a manner similar to **3a** but with higher affinity (−10.3 kcal/mol for **11a** and −10.6 kcal/mol for **11b** vs −10.0 kcal/mol for **3a** Fig. 2C and D, respectively). These fully unsaturated analogues (**11a** and **11b**) probably form H bonds with $Ser^{362}$ in the ligand binding pocket of MRSA PK, in a manner similar to the H bonding network of **3a** in MRSA PK.[3] Docking simulation using the reported conformation of **3a** showed H-bonds with chains A and B of MRSA PK, but the energy-minimized conformation of **3a** showed only a single H-bond with chain A of MRSA PK (Fig. 2B). Compound **11a** showed a H-bond with $Ser^{362}$ of chain A, whereas **11b** showed a H-bond with $Ser^{362}$ of chain B. The dibrominated analogue **11b** showed higher affinity than the monobrominated analogue **11a** possibly due to additional hydrophobic bromine interaction. The saturated analogues (**12**–**15**) were also speculated to form H bonds with $Ser^{362}$ in the ligand binding domain of MRSA PK in a similar manner as **3a** (see Supplementary data). However, their docking simulation affinities were lower than those of **11a** and **11b**. In general, analogues with a flat molecular skeleton showed higher affinity, presumably because they could more easily fit into the narrow gap between chains A and B. Therefore, we undertook to synthesize fully unsaturated and saturated analogues and to evaluate their antibacterial activities against MRSA and multidrug-resistant pathogens.

The synthesis of hamacanthin B derivatives commenced with 6-bromoindole (**5**), which was prepared using a typical method (Scheme 1).[12] 6-Bromoindole (**5**) was acylated using chloroacetyl chloride in pyridine to afford the chloride **6**, which was subsequently converted to the azide **7** in 85% yield by treating it with sodium azide in acetone–water. The azide **7** was easily converted into amine hydrochloride analogues by hydrogenation over Pd/C (palladium-on-carbon) in the presence of hydrochloric acid in methanol.[13] However, concurrent dehalogenation of these analogues by non-selective reduction, afforded a mixture of **8a** and **8b**, which was used in the next step without purification. Separately, 2-(6-bromo-1*H*-indol-3-yl)-2-oxoacetyl chloride (**9**) was prepared in 85% yield by refluxing 6-bromoindole (**5**) with oxalyl chloride in ether for 1 h, and used as a precursor for the synthesis of **10**.[14]

Reaction of **8a** and **8b** with 6-bromo-3-indolylglyoxylic chloride (**9**) gave a mixture of bisindolyl diketone amides (**10a** and **10b**). Pyrazinone ring formation was conducted by heating compounds **10a** and **10b** in an excess of ammonium hydroxide at 100 °C under high vacuum for three days to afford a mixture of the monobromo derivative **11a** and the dibromo derivative **11b**,[15] which was separated by reversed-phase HPLC. Reduction of the pyrazinones **11a** or **11b** with sodium cyanoborohydride produced the corresponding piperazinones (**12**–**15**), and the *cis*-isomers (**12** and **13**) were produced as major components (**12**:**14** = 1.4:1 for **11a** and **13**:**15** = 1.6:1 for **11b**). Diastereomeric mixtures were separated into *cis*- and *trans*-isomers by reversed-phase HPLC.[16]

*cis*-Isomers were identified based on the NOESY correlation between H-3 and H-5 (Fig. 3). Furthermore, the large coupling constant between H-5 and one H-6 ($J$ = 11.0 Hz, **13**) of the *cis* isomers indicated diaxial coupling in a chair conformation, conformers **A**/**A**′ with bulky indole rings at equatorial positions predominated, and that conformers **B**/**B**′ made negligible contributions (Fig. 3).

Isomers **14** and **15** did not show NOE correlation between protons H-3 and H-5. The $^1$H NMR spectra of **14** and **15** exhibited a notable difference from those of **12** and **13** with respect to the chemical shifts of piperazinone ring protons (H-3, H-5, and H-6). The signals of H-3, H-5, and that of H-6b were shifted upfield as compared with those of **12** and **13**. The $^{13}$C NMR spectra of these isomers were characterized by downfield shifts of C-3 and C-5, and an upfield shift of C-6 (**15**: $\delta$ 66.6 (C-3), 58.9 (C-5), 47.5 (C-6)) as compared to their *cis* counterpart (**13**: $\delta$ 58.2 (C-3), 51.6 (C-5), 49.1 (C-6)). Thereby, **14** and **15** were determined to be *trans*-isomers. The magnitude of the coupling constant between H-5 and H-6 ($J$ = 11.0 Hz, **15**) indicated diaxial coupling and a chair conformation of the piperazinone ring (Fig. 4). Therefore, conformers **A**/**A**′ with equatorially disposed H-3 and axially disposed H-5 prevailed. Steric hindrance between the C-2 carbonyl group and the C-3 indole ring of conformers **B**/**B**′ may have been responsible for the preference of conformers **A**/**A**′. The equatorial arrangement of the C-5 indole moiety would also stabilize conformers **A**/**A**′.

Racemic mixtures of the *cis*-isomers (**12** and **13**) and *trans*-isomers (**14** and **15**) were separated into individual enantiomers (**12a**/**12b**, **13a**/**13b**, **14a**/**14b**, and **15a**/**15b**) by chiral separation using a cellulose column and a hexane–EtOH mobile phase (see Supplementary data). The absolute configurations of the enantiomers with a *cis*-configuration (**12a**, **12b**, **13a**, and **13b**) were determined by optical rotation and ECD simulation. The specific rotation of **12a** (−14.4, *c* 0.15, MeOH) was of the same sign as that of the synthetic enantiomer (3*R*,5*S*)-*cis*-3,4-dihydrohamacanthin B (−92.3, *c* 0.2, acetone),[14] the specific rotation of **12b** (+22.1, *c* 0.3, MeOH) was of the same sign as that of natural (3*S*,5*R*)-6″-debromo-*cis*-3,4-dihydrohamacanthin B (**3d**, +105, *c* 0.2, MeOH;[5] +52.1, *c* 0.1, MeOH),[15] the specific rotation of **13a** (−40.2, *c* 0.11,